Molecular Therapy
Original Article

Human inhalable antibody fragments neutralizing SARS-CoV-2 variants for COVID-19 therapy

Olga Minenkova,[1] Daniela Santapaola,[1] Ferdinando Maria Milazzo,[1] Anna Maria Anastasi,[1] Gianfranco Battistuzzi,[1] Caterina Chiapparino,[1] Antonio Rosi,[1] Giuseppe Gritti,[2] Gianmaria Borleri,[2] Alessandro Rambaldi,[2,3] Clélia Dental,[4] Cécile Viollet,[4] Bruno Pagano,[5] Laura Salvini,[6] Emanuele Marra,[7] Laura Luberto,[7] Antonio Rossi,[8] Anna Riccio,[9] Emilio Merlo Pich,[1] Maria Gabriella Santoro,[8,9] and Rita De Santis[1]

[1]Alfasigma SpA, Biotechnology R&D, Via Pontina Km 30.400, Pomezia, 00071 Rome, Italy; [2]ASST Papa Giovanni XXIII, Piazza OMS, 1, 24127 Bergamo, Italy; [3]Department of Hematology and Oncology, University of Milan, Via Festa del Perdono, 7, 20122 Milan, Italy; [4]Texcell, Batiment Genavenir 5, Rue Pierre Fontaine 1, 91058 Evry Cedex, France; [5]Department of Pharmacy, University of Naples Federico II, Via Domenico Montesano, 49, 80131 Naples, Italy; [6]Fondazione Toscana Life Sciences, Via Fiorentina, 1, 53100 Siena, Italy; [7]Takis Srl, Via di Castel Romano, 100, 00128 Rome, Italy; [8]Institute of Translational Pharmacology, CNR, Via Fosso del Cavaliere, 100, 00133 Rome, Italy; [9]Department of Biology, University of Rome Tor Vergata, Via della Ricerca Scientifica, 1, 00133 Rome, Italy

As of December 2021, coronavirus disease 2019 (COVID-19), caused by the severe acute respiratory syndrome coronavirus 2 (SARS-CoV-2), remains a global emergency, and novel therapeutics are urgently needed. Here we describe human single-chain variable fragment (scFv) antibodies (76clAbs) that block an epitope of the SARS-CoV-2 spike protein essential for ACE2-mediated entry into cells. 76clAbs neutralize the Delta variant and other variants being monitored (VBMs) and inhibit spike-mediated pulmonary cell-cell fusion, a critical feature of COVID-19 pathology. In two independent animal models, intranasal administration counteracted the infection. Because of their high efficiency, remarkable stability, resilience to nebulization, and low cost of production, 76clAbs may become a relevant tool for rapid, self-administrable early intervention in SARS-CoV-2-infected subjects independently of their immune status.

INTRODUCTION

More than 2 years since the severe acute respiratory syndrome coronavirus 2 (SARS-CoV-2) pandemic began, although vaccination is starting to show its positive effect, the medical community is still urgently calling for novel, cost-effective therapeutic and prophylactic tools to control infection in non-immunized and in vaccinated subjects partially protected against emerging variants.[1–3] SARS-CoV-2 entry into cells is mediated by docking of the spike, a trimeric class I fusion protein anchored into the viral envelope, on the human angiotensin-converting enzyme 2 (hACE2),[4,5] and several spike-blocking anti-SARS-CoV-2 monoclonal antibodies (mAbs) are being sought for passive immunization.[6] Three mAbs received emergency use authorization (EUA) from the U.S. Food and Drug Administration (FDA) for the treatment of mild to moderate coronavirus disease 2019 (COVID-19) in non-hospitalized patients, and dozens are in clinical trials. Nevertheless, current evidence is still insufficient to draw meaningful conclusions regarding the utility of injected SARS-CoV-2-neutralizing mAbs,[7] whose widespread use is hampered by at least three limitations: first, loss of neutralization capacity toward emerging variants[8]; second, health system sustainability because of the costs of these products administered in gram doses and produced in expensive mammalian expression systems; and third, the risk for antibody-dependent enhancement (ADE) of the infection.[9] Additionally, recent data indicate that after the systemic infusion of a neutralizing mAb, SARS-CoV-2 is still present in the nasal turbinates,[10] where the virus initially harbors and from where it spreads, making intranasal and aerosol treatments particularly attractive.[11] Small, single-domain V_HH nanobodies, specific for SARS-CoV-2, were proposed for topical use (i.e., by inhalation) as an alternative to systemic mAbs.[12,13] However, being nanobodies of camelid origin, they require sophisticated humanization procedures to avoid immunogenic responses, potentially hampering their full development.[14]

Here we describe small human antibodies in the format of single-chain variable fragments (scFvs) that share several advantages with nanobodies with fewer risks.

RESULTS AND DISCUSSION

Selection of human scFv antibodies against SARS-CoV-2

ScFv antibodies were generated by engineering variable heavy- and light-chain sequences of immunoglobulins in a single polypeptide by joining them using a flexible peptide linker that allows reconstitution of the functional antigen-binding domains (Figure 1A).[15] Being devoid of immunoglobulin Fc, scFv antibodies are not at risk for inducing ADE, and because of their rapid production at large scale in non-mammalian expression systems, they could be developed at relatively lower cost compared with mAbs. Moreover, because of their smaller size (about 28 kDa vs the 150 kDa of mAbs) and low

Received 29 November 2021; accepted 9 February 2022;
https://doi.org/10.1016/j.ymthe.2022.02.013.

Correspondence: Rita De Santis, Alfasigma SpA, Biotechnology R&D, Via Pontina Km 30.400, Pomezia, 00071 Rome, Italy.
E-mail: rita.desantis@alfasigma.com

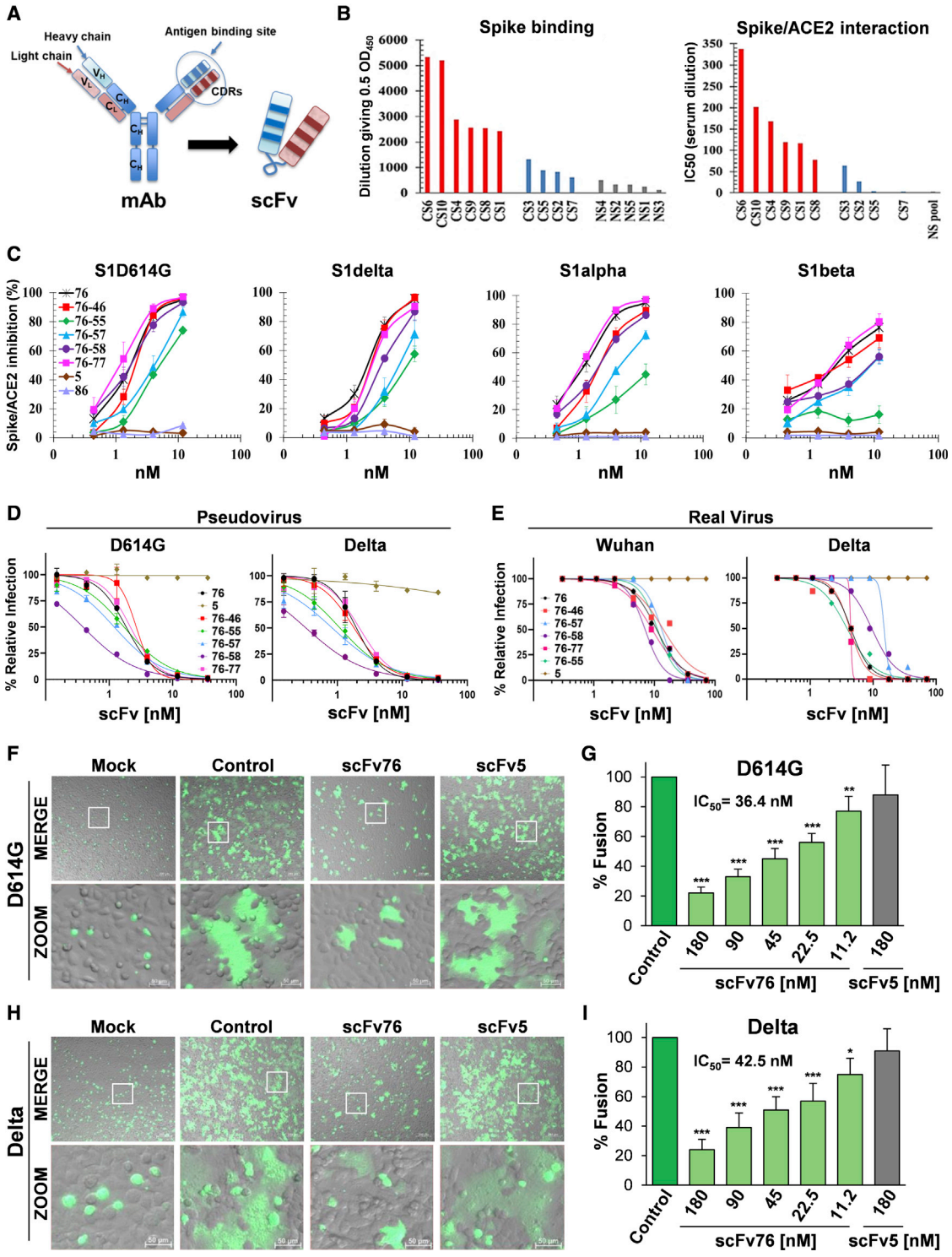

Figure 1. Selection and functional characterization of anti-SARS-CoV-2 human scFv antibodies

(A) Schematic representation of scFv and mAb.

(B) Analysis of COVID-19 convalescent (CS) and negative control (NS) sera for binding to SARS-CoV-2 spike (left) and inhibition of spike/hACE2 interaction (right) by ELISA. Data expressed as the dilution giving 0.5 OD and as IC_{50}, respectively.

(C) Inhibition of interaction of indicated spikes with hACE2 measured using ELISA. Data are the average ± SE of 2 or 3 experiments.

(legend continued on next page)

complexity (no glycosylation, simpler structure), they are particularly stable and suitable for topical use in non-hospital settings. For example, the first human scFv antibody, brolucizumab, was recently approved for topical treatment of exudative age-related macular degeneration by the FDA, thus paving the regulatory pathway for this class of molecules.[16]

SARS-CoV-2 neutralizing human scFv antibodies were obtained by panning phage display libraries on the spike receptor-binding domain (RBD). To maximize the possibility of selecting affinity-matured antibody species, we profiled the immune response to SARS-CoV-2 of ten COVID-19 convalescent donors from Papa Giovanni XXIII Hospital in Bergamo, Italy. As shown in Figure 1B (left panel), six out of ten COVID-19 sera (CS) were found to strongly bind to the SARS-COV-2 spike (Wuhan strain). These six sera also proved to be the most potent at inhibiting the spike-hACE2 interaction (Figure 1B, right panel) and the most effective at neutralizing viral infectivity in Vero E6 cells (Table S1). Total RNA, extracted from lymphocytes of the six best responders, was converted to cDNA, and the immunoglobulin genes were amplified and cloned in scFv antibody format for phage display, as depicted in Figure S1A. After selection cycles by panning, binders were subjected to affinity maturation by error-prone mutagenesis of the heavy chain and to light-chain shuffling followed by repeated panning on the RBD under stressing conditions (low antigen concentration, low-pH washing, high temperature). Selected scFv5, scFv86, and scFv76 antibodies, as well as affinity-matured derivatives from scFv76 (i.e., scFv76-46, scFv76-55, scFv76-57, scFv76-58, and scFv76-77), here coded as scFv76-cluster antibodies (76clAbs), all binding the SARS-CoV-2 spike in the sub- and low-nanomolar range, were produced in soluble form and purified according to the procedure schematized in Figure S1B. The amino acid sequences of CDR3 and germline gene repertoire of the selected scFv antibodies are reported in Table S2, which shows 76clAbs having identical VH CDR3 originating from the IGVH3-53 germline, with minor differences in the remaining VH sequence. Diversity is contributed by VL sequences that are derived from the IGVK3-20 germline, except for scFv76-55 and scFv76-57 antibodies, which originate VL from IGVK3-15 and IGVK1-9 germlines, respectively. Moreover, scFv5 and scFv86 antibodies share identical VH, derived from the IGVH1-46 germline, and have VL derived from the IGVL2-14 and IGVK3-11 germlines, respectively.

Human scFv antibodies neutralize SARS-CoV-2 variants

Recombinant spike S1-subunit and RBD-domain spike proteins of the SARS-CoV-2 variant of concern (VOC) delta and of variants being monitored (VBMs), all associated with high infectivity and immune escape, were then used to test scFv antibody reactivity in terms of binding, affinity, and inhibition of spike/hACE2 interaction. We included in the analyses spikes carrying the following mutations: D614G, here indicated as S1D614G, present now in all viral isolates; T19R, G142D, E156G, 157-158d, L452R, T478K, D614G, and P681R of the delta variant (S1delta); HV69-70del, Y144del, N501Y, A570D, D614G, and P681H of the alpha variant (S1alpha); and K417N, E484K, N501Y, and D614G of the beta variant (S1beta). RBD proteins with single or double mutations of most frequent variants were also tested. Results, shown in Figure S2 and Table S3, collectively indicate that 76clAbs strongly bind to mutated proteins and recognize much more efficiently all spikes and RBD mutated proteins compared with scFv5 and scFv86 antibodies that, on the basis of the pattern of reactivity, appear to recognize a different antigenic epitope. In a set of independent experiments, binding affinity of scFv antibodies for the SARS-CoV-2 spike was measured using surface plasmon resonance (SPR). Kinetic data on mutated spike and RBD proteins are reported in Table 1, Figures S3 and S4, and Table S4, showing K_D values ranging between sub-nanomolar and 1-digit nanomolar concentrations, except for scFv76-55, which exhibits a K_D of 14.9 nM for S1beta. SPR analyses did not reveal additive binding of the 76clAbs, suggesting that they might recognize the same or a very close antigenic epitope, while scFv5 binds to an independent epitope (Figure S5A). To test the ability of 76clAbs to recognize a SARS-CoV-2 native spike, HEK293T cells were transfected with the wild-type (WT) S1 spike-encoding plasmid. High-content screening (HCS) fluorescent imaging showed the scFv76 antibody binding to HEK293T spike + cells (Figure S5B). Similar data were obtained with all 76clAbs and confirmed on cytofluorimetry, indicating the ability of such antibodies to recognize the spike expressed on the cell surface (Figure S5C). The 76clAbs were then evaluated for their ability to inhibit the binding of the viral spike to hACE2 receptor and for their capacity to neutralize viral infectivity. Results in Figure 1C show that 76clAbs, but not scFv5 or scFv86, blocked spike/hACE2 interaction and that, except for scFv76-55, they were highly resilient to mutations of the delta variant, as well as to other mutations of VBMs (Figure S6). The half maximal inhibitory concentration (IC_{50}) values of 76clAbs, ranging from 0.36 to 4.30 nM, are reported in Table S5. ScFv5 and scFv86 antibodies did not interfere with spike or RBD binding to ACE2 at concentrations $\geq$40 nM. Interestingly, and consistent with binding and SPR affinity data, these results indicate that 76clAbs, except for scFv76-55, substantially maintain the capacity to inhibit the binding of the spike variants and mutated RBD to hACE2.

To investigate the potential escape of virus variants to 76clAb neutralization, infection of cells with pseudotyped as well as real viruses was

(D) Neutralization of pseudotyped virus expressing indicated spikes assessed by luciferase assay in hACE2-expressing Caco-2 cells. Data are the average ± SD of two replicates from one representative experiment.

(E) Microneutralization assay of SARS-CoV-2 Wuhan and delta strains in Vero E6 cells.

(F–I) Inhibition of SARS-CoV-2 spike-mediated cell-cell fusion using HEK293T donor cells expressing GFP and D614G-mutated (F and G) or delta (H and I) spike, or GFP only (mock), incubated 1 h with saturating dose (180 nM) of scFv76 or scFv5 (F and H) or with scalar doses of scFv76 (G and I), and then overlaid on monolayers of hACE2-expressing A549 cells for 4 h. The overlay of bright-field and fluorescence images is shown (MERGE). Scale bar, 200 μm; zoom, 50 μm. Cell-cell fusion quantification expressed as percentage relative to control (average ± SD of 5 fields from two biological replicates). *$p < 0.05$, **$p < 0.01$, and ***$p < 0.001$ (ANOVA).

Table 1. Affinity of anti-SARS-CoV-2 scFv antibodies for spike protein variants by surface plasmon resonance

scFv	Spike S1 variant	k_a (10^5 M^{-1} s^{-1})	k_d (10^{-5} s^{-1})	K_D (nM)
76	WT	1.4	4.7	0.3
	S1D614G	1.3	6.0	0.4
	S1alpha	1.1	4.3	0.4
	S1beta	1.3	54.0	4.1
	S1delta	1.0	6.6	0.7
76-46	WT	1.9	3.1	0.2
	S1D614G	1.9	4.8	0.3
	S1alpha	1.4	7.3	0.5
	S1beta	1.1	83.7	7.7
	S1delta	1.0	4.6	0.4
76-55	WT	1.4	42.1	3.0
	S1D614G	1.5	39.9	2.7
	S1alpha	1.2	61.6	5.1
	S1beta	1.5	223.0	14.9
	S1delta	1.0	54.2	5.6
76-57	WT	1.5	7.6	0.5
	S1D614G	1.5	6.7	0.4
	S1alpha	1.1	10.6	0.9
	S1beta	1.5	49.5	3.3
	S1delta	0.9	9.4	1.1
76-58	WT	2.8	32.6	1.1
	S1D614G	3.3	34.7	1.1
	S1alpha	2.8	34.0	1.2
	S1beta	1.7	75.0	4.5
	S1delta	1.8	37.6	2.1
76-77	WT	1.5	3.0	0.2
	S1D614G	1.4	4.9	0.3
	S1alpha	1.4	2.0	0.1
	S1beta	1.1	31.6	2.8
	S1delta	0.9	4.7	0.5
5	WT	0.5	19.8	4.3
	S1D614G	0.4	17.5	4.4
	S1alpha	0.5	19.8	4.2
	S1beta	0.5	20.0	4.1
	S1delta	0.3	15.8	4.9
86	WT	0.7	9.6	1.5
	S1D614G	0.6	11.4	1.8
	S1alpha	0.7	11.2	1.7
	S1beta	0.7	11.5	1.6
	S1delta	0.5	10.4	2.1

performed. The scFv5 antibody, which did not inhibit spike binding to hACE2, was selected as a negative control. Human colon Caco-2 cells stably expressing the hACE2 receptor (Caco-2 hACE2) were infected with luciferase-expressing SARS-CoV-2 S-pseudoviruses bearing the D614G mutation or the delta spike variant. Results in Figure 1D confirmed that 76clAbs, but not scFv5, inhibited the infection of both pseudoviruses as well as the infection of pseudoviruses bearing spike mutations of several VBMs (Figure S7A). Consistent with previous neutralization data, scFv76-55 was the least effective of the cluster and the most sensitive to mutations. Similar results were obtained comparing the neutralization potency of scFV76 and scFV76-55 on pseudoviruses bearing the alpha, beta, and gamma spike variants (Figure S7B).

Neutralization of infectivity of the real SARS-CoV-2 virus was then tested using microneutralization assay of cytopathic effect (CPE) in Vero E6 cells. Interestingly, all 76clAbs proved to be effective, with MN_{50} (50% microneutralization titer) < 15 nM against the delta variant (Figure 1E). Neutralization potency of scFv76, scFv76-46, and scFv76-58 antibodies was then further evaluated using qRT-PCR in human pulmonary Calu-3 cells infected with the SARS-CoV-2 Wuhan strain, D614G, or alpha variants. Results in Table S6 show that when the 76clAbs were added to the cell culture 1 h after the infection, they were effective at inhibiting all virus strains, with IC_{50} less than 22 nM, while when added 1 h before infection, the IC_{50} was less than 2.2 nM. A similar difference in the neutralization potency before or after infection was observed with the immune sera pooled from the six COVID-19 convalescent donors (Figure 1B; Table S1).

Human scFv antibodies counteract cell-cell fusion

The ability of 76clAbs to prevent SARS-CoV-2 spike-induced fusion of pulmonary cells was tested *in vitro* (Figure S8A). This analysis has high translational value, as syncytia formation in the lung is considered a most relevant pathologic hallmark of COVID-19, driving localized inflammation and thromboembolism.[17] Incubation with nanomolar concentrations of the scFv76 antibody proved to be strongly effective at inhibiting fusion between WT (Wuhan) (Figures S8B and S8C), D614G (Figures 1F and 1G), and delta (Figures 1H and 1I) spike-expressing human HEK293T cells and human lung A549 cells stably expressing the hACE2 receptor (A549 hACE2). These observations were replicated in monkey Vero E6 target cells (Figure S8C).

Epitope mapping

Identification of the antigenic epitope recognized by anti-SARS-CoV-2 scFv antibodies was performed using high-throughput flow cytometry on human HEK-293T cells expressing Wuhan or alanine-mutated RBD proteins (alanine scanning library of 194 aa). Data in Figure 2A show, for scFv76, scFv76-55, scFv76-57, scFv76-58, and scFv86, cytofluorimetry dot plots indicating primary (red) and secondary (blue) critical clones bearing alanine substitutions in positions strongly reducing binding. Such critical residues (red and blue spheres) are visualized on a crystal of the SARS-CoV-2 spike protein trimer (PDB: 6XCN) and the SARS-CoV-2 spike protein receptor-binding domain (PDB: 6Z2M). Results indicate that 76clAbs recognize an epitope on the spike RBM that includes F456, Y473,

N487, and Y489 residues, while the critical residue for the non-neutralizing scFv86 is mapped outside the RBM. Interestingly, none of the residues composing the epitope recognized by 76clAbs has been found mutated neither in the delta VOC or in the VBMs. During the preparation of the present report, the omicron variant emerged and was recently classified as a new VOC. Omicron bears 15 mutated RBD residues, and it has been found to be able to escape neutralization by immune sera as well as by the majority of approved and investigational anti-RBD monoclonal antibodies.[18,19] It is remarkable that, despite such a large number of mutations, all the residues composing the epitope recognized by 76clAbs are conserved in omicron (Figure S9).

Taking together the alanine scanning and the functional data shown above, it is possible to speculate that the epitope recognized by 76clAbs might be invariant because, being structurally located at the tip of the spike, its conformation is essential for the docking to hACE2. This epitope was found to be restricted to SARS-CoV-2, as indicated by lack of reactivity of 76clAbs with SARS-CoV, Middle East respiratory syndrome coronavirus (MERS-CoV), and HCoV-HKU1 spikes (Figure 2B). Overall, the data collected so far on the functional profiles of 76clAbs together with the epitope mapping collectively show that the reactivity of these antibodies is not affected by mutations present in SARS-CoV-2 variants, including those previously found to be associated to the escape of antibody recognition.[8,18–21]

Biochemical characterization of human anti-SARS-CoV-2 scFv antibodies

Regarding the biochemical properties of 76clAbs, size exclusion chromatography-high-performance liquid chromatography (SEC-HPLC) and SDS-PAGE electrophoresis (Figures 3A and S10) indicated an apparent molecular weight of about 28 kDa, as expected on the basis of deduced amino acid sequence. Molecular weight was further confirmed by SEC-HPLC-mass spectrometry (MS) using 20 mM ammonium formate as native elution buffer. The average spectrum obtained from all MS spectra of the scFv76 antibody is reported in Figure 3B, in which two Gaussian dispersions, centered on m/z 2800 and m/z 4000, are present. Their deconvolution indicates the presence of two species with molecular weights of 28,008 and 56,016 that correlate with the scFv76 monomeric and dimeric forms, respectively. The results of peptide mapping performed by trypsin digestion of scFv76, scFv76-46, scFv76-58, and scFv76-77, followed by reverse-phase-ultra-HPLC-MS/MS analysis, confirmed 100% matching of peptides with the expected amino acidic sequence. Thermal resistance, selected as a surrogate marker of protein stability, was then investigated. The 76clAbs were subjected to heating for 1 h at increasing temperature and tested for RBD binding using ELISA. Results in Figure 3C identify scFv76, scFv76-46, and scFv76-58 as the most resistant antibodies and scFv76-57 as the most sensitive. To assess protein folding and secondary structure content, far-UV circular dichroism (CD) spectra of 76clAbs were recorded at 20°C and 90°C (Figure 3D). CD spectra of antibodies at 20°C resemble those of folded proteins with significant β-sheet content, while the spectra at 90°C show that the antibodies have undergone unfolding. Quantitative analysis of CD spectra at 20°C, by means of BeStSel,[22] indicates that 76clAbs have a folded structure with about 40% of antiparallel β-sheet content (Table S7). Considering the possible use of the 76clAbs for aerosol therapy of COVID-19, their resilience to nebulization stress was also evaluated. The results obtained show that aqueous solutions of scFv76, at milligram/milliliter concentrations, can be nebulized by a mesh nebulizer, maintaining unaltered both protein integrity (Figure 3E) and spike binding property (Figure 3F).

Intranasally administered scFv antibodies inhibit SARS-CoV-2 infection in animal models

The *in vivo* effect of the topical administration of various members of 76clAbs against SARS-CoV-2 infection was then investigated in a model of hACE2-expressing transgenic (tg) mice, infected with a luciferase-expressing D614G S-pseudotyped virus. Infection in nasal turbinates was measured using bioluminescence imaging (BLI). As shown in Figure 4A, the intranasal administration of 74 μg/mouse of scFv76 (37 μg/nostril), 2 h before and 4 h after infection, completely blocked the viral infection, as deduced by the loss of luminescent signal (Figure 4B). In a confirmatory study, scFv76-58 and one unrelated scFv antibody were also tested. Results, shown in Figure 4C, confirmed the efficacy of both 76clAbs, while the unrelated antibody was not active, thus indicating treatment specificity. In an independent study, hamsters, one of the few animals sensitive to human SARS-CoV-2, were infected with the D614G SARS-CoV-2 strain. Hamsters were intranasally administered with 70 μg of scFv76 (35 μg/nostril), 2 h before and once daily for the 2 consecutive days post-infection. Results showed protection from body weight loss (Figure 4D) and reduction of nasal discharge (Figure 4E). Finally, a propaedeutic investigation of scFv76 aerosol delivery (Figure S11A) was performed by nose-only exposure of mice to antibody solutions nebulized by the Aerogen Pro (Aerogen) mesh nebulizer, a nebulization device used for human treatment. Results in Figure S11B indicated that nebulized scFv76 antibody can be effectively delivered to the lung down to the alveolar space, as shown by immunohistochemistry. The amount of antibody deposited appears to increase with time of exposure, as shown by tissue staining intensity (Figure 4F) and by RBD binding ELISA of homogenized lungs (Figure 4G).

Because of reported SARS-CoV-2 molecular mimicry of human proteins and related extensive cross-reactivity of anti-virus antibodies with human normal tissues,[23] scFv76 was tested by immunohistochemistry on tissue microarrays (Figure S12A). Representative pictures in Figure S12B clearly show reactivity of an anti-PDL1 scFv antibody (generated using the same technology as scFv76 and equally detected by anti-His tag antibodies) with several tissues, while no reactivity was observed with scFv76, thus confirming its suitability as a potential drug for human use.

In summary, here we describe a class of anti-SARS-CoV-2 human scFv antibodies endowed with sub-nanomolar neutralization potency, *in vivo* efficacy, and significant stability. These small, fully human antibodies are expected to be well tolerated and be produced at

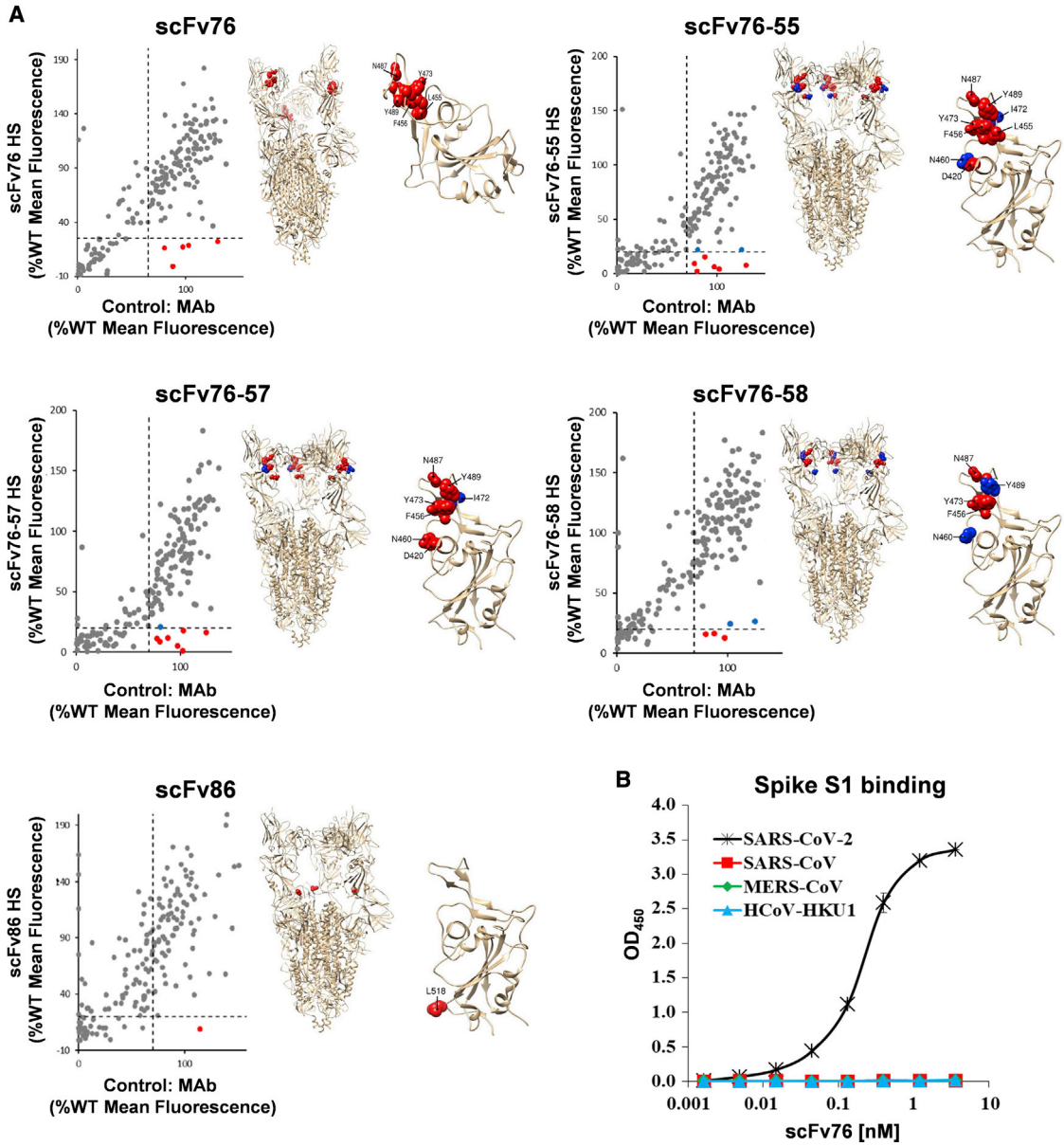

Figure 2. Epitope mapping of anti-SARS-CoV-2 human scFv antibodies

(A) Flow cytometry dot plot representation of antibody binding to alanine-mutated clones (left). For each point, background fluorescence was subtracted from the raw data, which were then normalized to reactivity with WT target protein. To identify preliminary primary critical clones (red circles), a threshold (dashed lines) of >65% WT binding to control Ab and <25% WT binding to test Abs was applied. Secondary clones (blue circles) are highlighted for clones that did not meet the set thresholds but whose decreased binding activity and proximity to critical residues suggested that the mutated residue may be part of the antibody epitope. Critical residues (red spheres) for scFv antibodies binding, and secondary residues (blue spheres) that may contribute to binding, are also visualized on crystal structure of the SARS-CoV-2 spike protein trimer (PDB: 6XCN) (center) and on SARS-CoV-2 spike protein receptor-binding domain (PDB: 6Z2M) (right).

(B) Reactivity of scFv76 toward indicated spikes by ELISA.

low cost and thus are promising candidates for early treatment of COVID-19. Remarkably, the ability of 76clAbs to recognize an essential and conserved spike antigenic epitope translates into the neutralization of the delta variant and the VBMs identified thus far, some of which are known to drive escape of approved and investigational mAbs.[24] The single-chain antibodies here proposed for nasal or lung topical delivery might overcome limitations of parenteral mAbs aimed at systemic passive immunization.[25] Developed as a complementary approach to existing vaccination and passive systemic immunization, which do not induce a robust mucosal

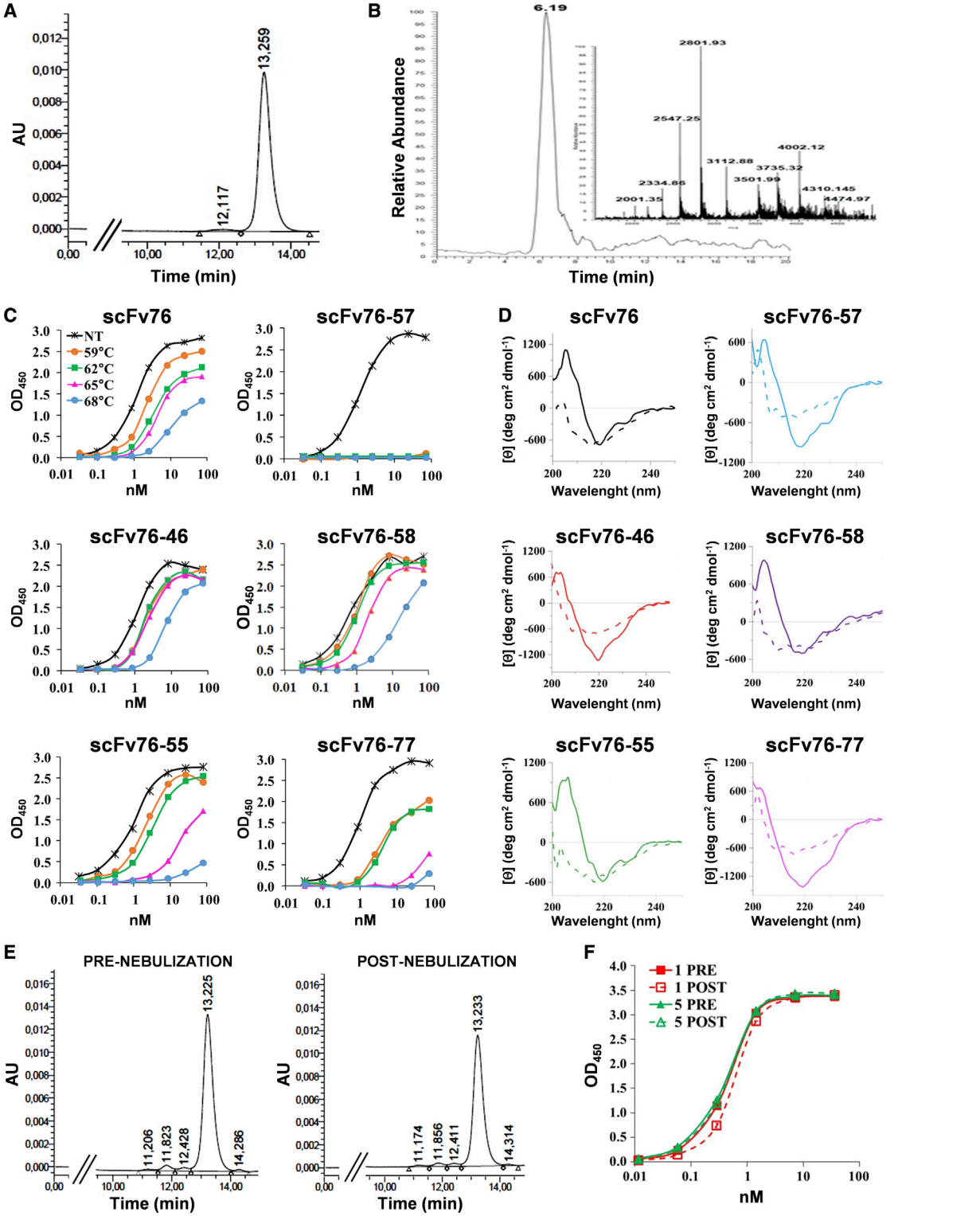

Figure 3. Biochemical and structural characterization of 76clAbs

(A) UV chromatogram at 280 nm from SEC-HPLC analysis of scFv76 in 50 mM phosphate buffer, 150 mM NaCl, 10% acetonitrile (pH 7.2) on TSKgel G3000 SWXL 30 cm × 7.8 mm column (Tosoh Bioscience).

(legend continued on next page)

defense,[26] this class of antibodies may contribute to halt the SARS-CoV-2 infection in its early stages.

MATERIALS AND METHODS

Convalescent sera and RNA

Total RNA was purified from 10 mL peripheral blood from ten COVID-19 convalescent subjects, confirmed virus free by double-negative swab, among the personnel of ASST Papa Giovanni XXIII Hospital of Bergamo. Matched sera from each donor were also provided. All samples were anonymized, and donors consented to the use of their biological materials for the generation of phage libraries displaying antibodies on their surface, according to a protocol approved by the ethics committee.

Phage libraries

Total RNA was converted to cDNA by using Super Script IV VILO Master Mix (Thermo Fisher Scientific). For library construction, cDNAs derived from lymphocytes of the best 6 responders (CV1, CV4, CV6, CV8, CV9, and CV10) were used. Gene fragments encoding for immunoglobulin variable domain were amplified with specific primers and assembled into scFv antibody genes as described earlier.[27] The libraries of scFv format were prepared by inserting assembled scFv genes in the proprietary vector pKM19.[28,29] Each library had an average size of about 5×10^7 independent clones. Maturation libraries were generated on the base of originally selected clones by error-prone PCR amplification of heavy chains and by light-chain shuffling. Heavy-chain DNA fragment of the chosen clones was amplified with upstream vector primer and 3′-end VH primer. To introduce a low rate of mutations in the heavy chains under error-prone amplification, the following conditions were used: 1 mM dTTP, 1 mM dGTP, 1 mM dCTP, 0.2 mM dATP, 0.1 mM dITP, 7 mM $MgCl_2$ (including $MgCl_2$ from Taq buffer), and 0.5 mM $MnCl_2$. The mutated VH DNA sequences were assembled with sequences encoding the whole repertoire of VL by introducing between the two chains a short linker of 15 amino acids $(GGGGS)_3$,[15] and scFv encoding sequences were cloned in pKM19.

ScFv selection

About 5×10^{11} TU (transducing units) of freshly amplified scFv antibody library were preincubated, in blocking buffer, with 10% of human serum, 10% AD202 bacterial extract, and 10% UV-killed M13KO7 for 30 min at 37°C. Fifty microliters of protein G conjugated Dynabeads were incubated with 2 μg SARS-CoV-2 RBD human Fc for 30 min at room temperature (RT) with slow agitation, then washed, blocked with complete blocking buffer, and added to the library and incubated for 1 h at 37°C under gentle agitation. The bound phage was captured by using a magnetic concentrator, washed ten times with PBS/Tween (PBS, 0.1% Tween 20), and then eluted by 0.1 M glycine (pH 2.2) for 10 min at RT and then neutralized by 2 M Tris (pH 9.6). Conditions of selection of matured clones were designed to be more stringent. The phage suspension was incubated for 1 h at 63°C before adding to the antigen-coated carrier. Moreover, bound phages were intensively washed with washing buffer 10 times and additionally with 0.1 M glycine (pH 4.0) before elution. Once identified, the scFv genes were re-cloned in pKM16[28] for production of soluble antibodies.

Lab-scale production and purification of soluble scFv

A plasmid DNA encoding for scFv antibody was used to transform *E. coli* DH5αF′ cells. A single colony was inoculated in 50 mL LB containing 100 μg/mL ampicillin and 2% glucose and incubated at 37°C overnight (ON). Next day, 10 mL of bacterial suspension were inoculated in 1 L LB containing 2% glucose and 100 μg/mL ampicillin. The cells were grown up to OD 0.8. Bacteria were then collected using centrifugation. The pellet was resuspended in 1 L LB containing ampicillin and 20 mM $MgCl_2$ and incubated for further 4.5 h at 30°C. Bacteria were collected, and the pellet was resuspended in 100 mM Tris-HCl (pH 7.4) and 10 mM EDTA for periplasmic protein extraction and incubated ON at 30°C with agitation. Cell debris was removed, and the supernatant was subjected to filtration by using Cogent μScale Tangential Flow Filtration System. Buffer was exchanged to 20 mM phosphate buffer (pH 7.4) and supplemented with 25 mM imidazole, and volume was reduced to 50 mL. His-tagged scFv was purified by using a HisTrap crude prepacked ready-to-use column operating with AKTA Avant liquid chromatography system (GE). The antibody was further purified from endotoxins by using Triton X-114. To purify solution from residual Triton X-114, Pierce Detergent Removal Spin Columns (Thermo Fisher Scientific) were used, according to the manufacturer's instruction. Samples were then filter-sterilized and stored in aliquots at −80°C.

Binding to spike or RBD and ACE2 binding competition

For binding experiments, Nunc MaxiSorp plates with 96 wells were coated with 100 μL/well SARS-CoV-2 spike S1 (SARS-CoV-2 spike glycoprotein S1 sheep Fc-tag, His-tagged spike S1 [D614G], spike S1[HV69-70del/Y144del/N501Y, A570D, D614G, P681H], spike S1 [K417N, E484K, N501Y, D614G], spike S1 [T19R, G142D, E156G, 157-158 deletion, L452R, T478K, D614G, P681R]] or His-tagged RBD proteins WT or with single or double mutation at K417, N439, L452, Y453, I472, A475, T478, V483, E484, N501, and A520 (all from Sino Biological) in PBS, at a final concentration of 0.5 μg/mL, ON at +4°C. Plates were blocked with blocking solution (1%

(B) Total ionic current (TIC) chromatogram from SEC-HPLC analysis of scFv76 in 20 mM ammonium formate (pH 6.8) on Mab Pac SEC-1 column (Thermo Fisher Scientific). Inset: mass spectrum as average of spectra recorded between 5 and 7 min.

(C) Binding to SARS-CoV-2 RBD of thermally stressed (1 mg/mL concentration for 1 h at indicated temperatures) and not treated (NT) 76clAbs by ELISA. Data from one representative experiment.

(D) Far-UV circular dichroism spectra of antibodies. Analysis was performed in PBS buffer at 20°C (solid lines) and 90°C (dashed lines).

(E) UV chromatograms at 280 nm from SEC-HPLC analysis, as in (A), of scFv76 pre- and post-nebulization at 1 mg/mL.

(F) Binding of scFv76, pre- and post-nebulization at 5 or 1 mg/mL, to SARS-CoV-2 RBD by ELISA. Data are from one representative experiment.

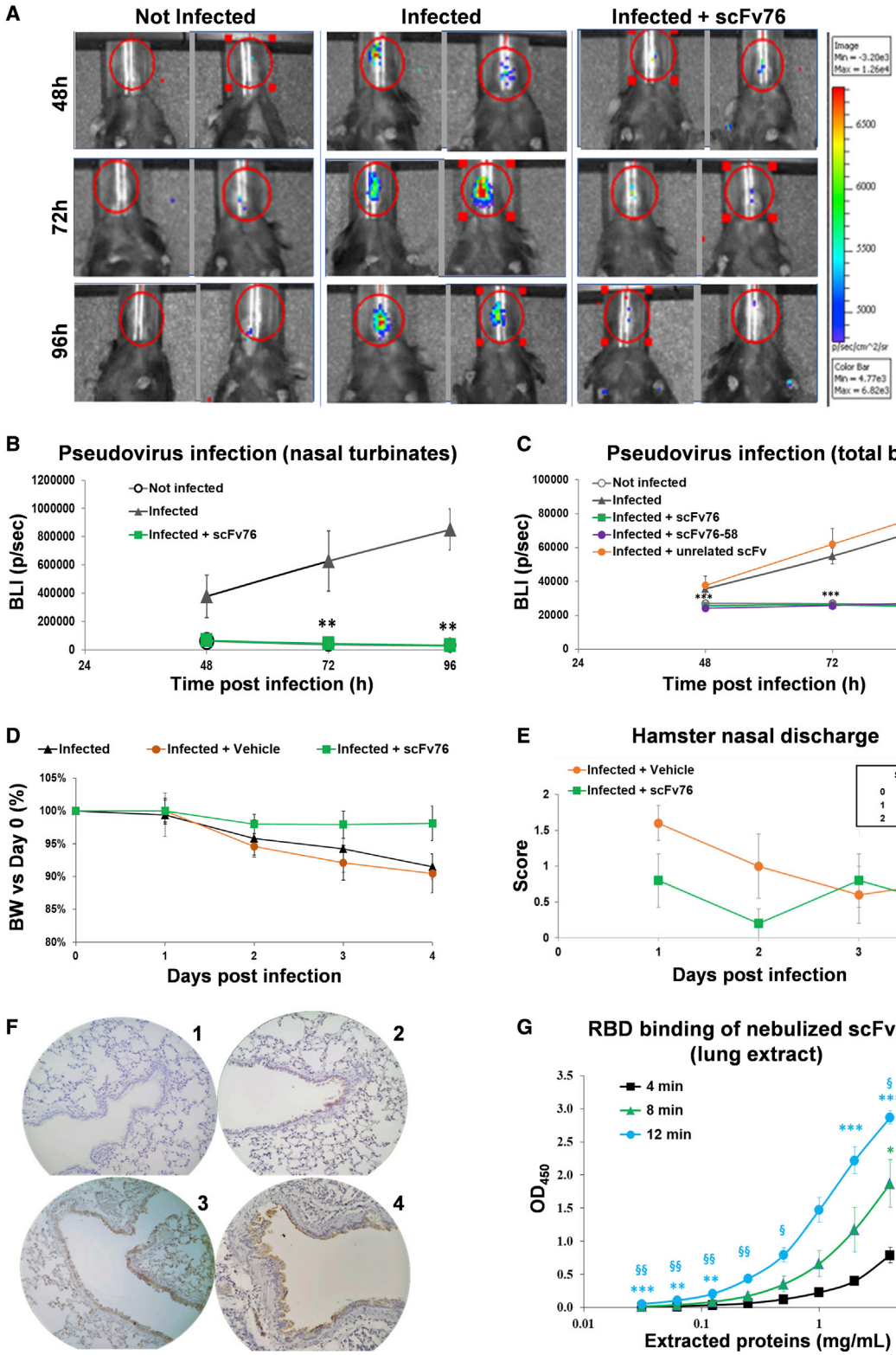

(legend on next page)

BSA in PBS/Tween) for 2 h at RT. After washing, dilutions of antibodies were added in a volume of 100 µL/well and incubated for 1 h at 37°C. Plates were washed 4 times with PBS/Tween and incubated for 1 h at RT with 100 µL/well of an anti-FLAG horseradish peroxidase (HRP)-conjugated antibody (Sigma-Aldrich) diluted 1:5,000 in blocking buffer. After 4 washings with PBS/Tween, 100 µL/well TMB substrate was added and plates were incubated at RT in the dark. The reaction was stopped by adding 50 µL 2 N H_2SO_4. Absorbance was recorded at 450 nm using a SUNRISE spectrophotometer (TECAN).

Similar experiments were performed to assess the binding specificity of 76clAbs by using SARS-CoV spike/S1, MERS-CoV spike/S1, or HCoV-HKU1 spike/S1 His-tagged proteins (all from Sino Biological).

For competition experiments, Nunc MaxiSorp plates with 96 wells were coated with 100 µL/well of spike S1 (SARS-CoV-2 spike glycoprotein S1 sheep Fc-tag, His-tagged spike S1 [D614G], spike S1 [HV69-70del/Y144del/N501Y, A570D, D614G, P681H], spike S1 [K417N, E484K, N501Y, D614G], spike S1 [T19R, G142D, E156G, 157-158 deletion, L452R, T478K, D614G, P681R]) or His-tagged RBD proteins WT or with single or double mutation at K417, N439, L452, Y453, I472, A475, T478, V483, E484, N501, and A520 (all from Sino Biological) in PBS, at a final concentration of 1.0–0.25 µg/mL, ON at +4°C. Plates were blocked with 300 µL/well blocking solution for 2 h at room temperature. After washing, dilutions of antibodies were added in a volume of 50 µL/well at double concentration, and after 30 min incubation at 37°C, 1.0–0.25 µg/mL human ACE2 protein mouse Fc-tag (Sino Biological) was added and incubated for 1 h at 37°C. Plates were washed 4 times with PBS/Tween and then incubated for 1 h at RT with 100 µL/well of an anti-mouse Fc conjugated to alkaline phosphatase (Sigma-Aldrich), diluted 1:1,000 in blocking buffer. After 4 washings, 100 µL/well pNpp substrate was added and plates were incubated at RT in the dark. Absorbance was recorded at 405 nm using a SUNRISE spectrophotometer.

Surface plasmon resonance

Kinetic constants were determined using SPR experiments with a Biacore T200 instrument (Cytiva). Wuhan strain SARS-CoV-2 spike S1 mouse Fc-tagged protein (Sino Biological; 5 µg/mL in acetate buffer, pH 5), mutated SARS-CoV-2 spike S1 His-tagged proteins (Sino Biological; 5 µg/mL in acetate buffer, pH 5), and SARS-CoV-2 RBD His-tagged proteins (Wuhan strain and mutated ones; Sino Biological; 2.5 µg/mL in acetate buffer, pH 5) were immobilized at 350 RU level (S1 proteins) and at 100 RU level (RBD proteins) on the surface of a flow cell of a Series S sensor chip CM5 (Cytiva) using the classical amine coupling procedure, while another flow cell surface was blank-immobilized with ethanolamine to be used as control surface. Then scFv proteins were flowed at 30 µL/min on both flow cells at 0.47, 1.40, 4.19, 12.56, 37.67, and 113 nM concentrations in HBS-EP + buffer (Cytiva) for a contact time of 480 s. After a dissociation time of 900 s (1,500 s for scFv76-77), both flow cells surfaces were regenerated by flowing 10 mM glycine-HCl (pH 1.5) at 30 µL/min for 30 s and 10 mM NaOH at 30 µL/min for 30 s. Double referenced sensorgrams were obtained by subtraction of blank-immobilized flow cell curves, as well as of zero concentration curves, from derivatized surface flow cell curves. Kinetic constants were obtained by BIAevaluation 3.2 software (Cytiva) fitting with a 1:1 binding model. For binning experiment by SPR, SARS-CoV-2 RBD mFc-tagged (Sino Biological; 10 µg/mL in acetate buffer, pH 5) was immobilized at 300 RU level on the surface of a flow cell of a Series S sensor chip CM5 (Cytiva) using the classical amine coupling procedure, while another flow cell surface was blank-immobilized with ethanolamine to be used as control surface. Eight scFvs (76, 76-77, 76-58, 76-57, 76-55, 76-46, 86, and 5) were sequentially flowed on both surface at 100 nM in HBS-EP+ (Cytiva) with a contact time of 600 s and a dissociation time of 60 s for each protein, except for the last one (scFv5), which was allowed to dissociate for 240 s. Then both flow cells surfaces were regenerated by flowing 10 mM glycine-HCl (pH 1.5) at 30 µL/min for 30 s and 10 mM NaOH at 30 µL/min for 30 s. A double referenced sensorgram was obtained by subtraction of blank-immobilized flow cell curve, as well as of sequentially zero concentration curve, from derivatized surface flow cell curve.

HCS fluorescence imaging (Operetta)

Human embryonic kidney HEK293T cells stably expressing the SARS-CoV-2 spike glycoprotein S1 (generated by transfection with plasmid DNA encoding for S1 protein and subsequent clonal selection) were seeded in 96-well microtiter plates (5×10^5 cells/well) pretreated with polyethyleneimine (Sigma-Aldrich). After 24 h, cells were washed with PBS, fixed with 4% formaldehyde, permeabilized with PBS/Tween (PBS, 0.2% Tween 20), and blocked with 2% BSA

Figure 4. Intranasally administered scFv76 antibody inhibits viral infectivity in animal models

(A) Representative bioluminescence images (BLI) at different time points after intranasal administration of scFv76 in K18-hACE2 mice infected with a luciferase-expressing SARS-CoV-2 spike (D614G) pseudotyped virus. Imaging by Xenogen IVIS200.

(B and C) BLI photons/sec in nasal turbinates (B) and (C) total body. BLI data expressed as average ± SE of 5 animals. **$p < 0.01$ and ***$p < 0.001$, Student's t test versus infected (vehicle-treated) mice.

(D and E) Body weight (D) and (E) nasal discharge of hamsters intranasally infected with SARS-CoV-2 (D614G) 10^5 pfu/animal on day 0 (D0) and treated with ScFv76 or vehicle 2 h before and once daily for 2 days post-infection. Body weight expressed as percentage versus D0. Nasal discharge scored as in the inset. Data are average ± SD of 5 animals/group.

(F) Immunohistochemistry of pulmonary sections of mice, 1 h after PBS (panel 1) or 1 h after 4 min (panel 2), 8 min (panel 3), or 12 min (panel 4) scFv76 (5 mg/mL solution) aerosol exposure.

(G) SARS-CoV-2 RBD binding by ELISA of lung proteins extracted from mice as in (F). Data expressed as average ± SD (n = 4). *$p < 0.05$, **$p < 0.01$, and ***$p < 0.001$, Student's t test versus 4-min-nebulized mice. §$p < 0.05$ and §§$p < 0.01$, Student's t test versus 8-min-nebulized mice.

in PBS/Tween. Cells were then incubated with 50 µL/well scFv at concentration of 10 µg/mL, for 1 h at 4°C. After three washings with PBS/Tween, plates were treated with 10 µg/mL of a mouse anti-FLAG M2-FITC (Sigma-Aldrich). Cells were ultimately counterstained with Draq5 (Axxora) and analyzed for fluorescence using the high-content screening system Operetta (PerkinElmer).

Flow cytometry analysis

Human embryonic kidney HEK293T cells stably expressing the SARS-CoV-2 spike glycoprotein S1 (generated by transfection with plasmid DNA encoding for S1 protein and subsequent clonal selection) were washed with PBS and incubated with 360 nM scFv for 1 h at 4°C. After three washings with PBS, cells were treated with 10 µg/mL of a mouse anti-FLAG M2-FITC (Sigma-Aldrich), washed again, and analyzed for fluorescence using an ATTUNE NxT acoustic focusing cytometer (Invitrogen/Thermo Fisher Scientific). Dead cells were ruled out from the analysis using propidium iodide staining (P4864; Sigma Aldrich).

Microneutralization assay

Neutralizing antibody titers were tested using a live-virus assay as follows. Decomplemented serum or scFv samples were pre-diluted in inoculation medium (DMEM, 2% fetal calf serum, 1% glutamine), followed by 9 serial dilutions in inoculation medium. Serial dilutions were then mixed 1:1 with 2,000 $TCID_{50}$/mL SARS-CoV-2 virus (strain 2019-nLOV/Italy INM1 or strain hCoV-19/USA/PHC658/2021 [B.1.617.2] WCCM) and incubated for 1 h at +37°C in 5% CO_2. Then 35 µL of each dilution/virus mix was applied in octuplicate to Vero E6 cells seeded at a density of 10^5 cells/mL in a 96-well plate at day −1. After 1 h incubation at 37°C in 5% CO_2, 65 µL culture medium (DMEM, 2% fetal calf serum, 1% glutamine) was added to each well. Plates were incubated for 4 days at 37°C in 5% CO_2. After this period, cells were inspected for cytopathic effect, and the number of CPE-positive wells was recorded. The titer at which no CPE was observed in at least half of the octuplicates (50% microneutralization titer) was calculated according to the Spearman-Kärber formula[30] for each sample.

Viral neutralization in Calu-3 cells

To measure the SARS-CoV-2-neutralizing capability of antibodies and patient sera, a live SARS-CoV-2 assay was performed by measuring the viral load in human lung adenocarcinoma Calu-3 cells, by real-time qRT-PCR, 72 h after virus infection. The experiments were carried out at the François Hyafil Research Institute (Oncodesign, Villebon-sur-Yvette, France). Calu-3 cells were seeded in 96-well plates in complete cell culture medium (MEM + 1% pyruvate + 1% glutamine + 10% fetal bovine serum) and then infected, at a multiplicity of infection of 0.01, with three different SARS-CoV-2 virus strains: the SARS-CoV-2, 2019-nCoV/Japan/TY/WK-521/2020 strain, the Slovakia/SK-BMC5/2020 strain (endowed with the D614G mutation), and the Slovakia/SK-BMC-P1A/2021-B.1.1.7 variant (VOC 202012/01) strain (U.K. origin). Antibodies and a pool of patient sera were assessed in two different approaches. In the first one, 1 h after infection the virus solution was discarded and replaced by a volume of growth medium containing each test compound, in a concentration ranging from 214 to 2.6 nM (or at dilutions from 1/20 to 1/320 for sera), in triplicate. In the second approach, test antibodies (in a concentration ranging from 214 to 0.097 nM) and sera (at the same dilutions as above) were premixed with the virus 1 h at room temperature and then added to cells. The plates were then transferred in a 37°C incubator for 72 h. Finally, the cell culture supernatants were collected for viral RNA extraction (Macherey Nagel Viral RNA kit), and viral RNA copy number was quantified using qRT-PCR, targeting a region in the IP2/IP4 gene and using a CFX384 Real-Time PCR Detection System (Bio-Rad Laboratories). Data were processed using GraphPad Prism software (version 8.0), and the IC_{50} values calculated using a four-parameter logistic curve fitting approach.

Cell-cell fusion assay

Human alveolar type II-like epithelial A549 cells, embryonic kidney 293T cells, and monkey kidney Vero E6 cells were obtained from ATCC (Manassas, VA). Cells were grown at 37°C and 5% CO_2, in RPMI-1640 (A549 cells) or DMEM (Vero E6 and 293T cells) medium (Euroclone) supplemented with 10% fetal calf serum (FCS), 2 mM glutamine, and antibiotics. Generation of A549 cells stably expressing the human ACE2 receptor (A549-hACE2 cells) has been described previously.[31] The C-terminal FLAG-tagged pCMV3-2019-nCoV-spike (S1+S2)-long-FLAG (SARS-2, Wuhan) and the pCMV3-SARS-CoV-2-spike (S1+S2)-long (B.1.617.2) (delta) vectors were obtained from Sino Biological. FLAG-tagged pCAGGS-SARS2-S-G614 (Addgene plasmid #156421) (D614G) vector was a gift from Hyeryun Choe and Michael Farzan.[32] The pCMV-GFP vector was obtained from Clontech. Transfections were performed using Lipofectamine 2000 (Invitrogen, Thermo Fisher Scientific), according to the manufacturer's instructions. In the donor-target cell fusion assay, 293T cells were co-transfected with plasmids encoding the FLAG-tagged SARS-CoV-2 Wuhan S-protein, the FLAG-tagged D614G S protein, or the spike protein from the SARS-CoV-2 Delta variant, and GFP. 293T cells, co-transfected with the GFP-encoding plasmid and the empty vector, were used as negative control. At 40 h post-transfection, cells were detached with trypsin (0.25%) and incubated with different concentrations of scFv76 or scFv5 antibodies at 37°C. After 30 or 60 min, cells were overlaid on an 80% confluent monolayer of target cells (Vero E6 [naturally expressing ACE2 receptors on the membrane surface] or A549-hACE2 [stably transfected with the hACE2 encoding plasmid] cells) at a ratio of approximately one S-expressing cell to three receptor-expressing cells.[33] After 4 h, nuclei were stained with Hoechst. Transmission and fluorescence images were taken using a Zeiss Axio Observer inverted microscope. To measure the extent of cell-cell fusion, the GFP area was delimited, measured using ImageJ software,[34] divided by the total cell area, and expressed as percentage relative to control. Images shown in all figures are representative of at least five random fields (scale bars are indicated). Statistical analysis was performed using one-way ANOVA (Prism 6.0 software; GraphPad). All experiments were done in duplicate and repeated at least twice.

Generation of SARS-CoV-2 S-pseudoviruses

Embryonic kidney 293T cells (ATCC) were grown at 37°C and 5% CO_2, in DMEM (Euroclone) supplemented with 10% FCS, 2 mM glutamine, and antibiotics. The C-terminal FLAG-tagged pCMV3-2019-nCoV-spike (S1+S2)-long-FLAG (Wuhan) and pCAGGS-SARS2-S-G614 (Addgene plasmid #156421) (D614G), and the pCMV3-SARS-CoV-2-spike (S1+S2)-long (B.1.617.2) (delta) vectors are described above. The mutants N501Y and K417N + E484K + N501Y were constructed on the Wuhan plasmid; mutations were generated and sequence-validated by Bio-Fab Research (Rome, Italy). The C-terminal FLAG-tagged pReceiver-M39 UK B.1.1.7 (EX-CoV242-M39) (alpha), South Africa B.1.351 (EX-CoV244-M39-GS) (beta), and Brazil B.1.1.28 (EX-CoV245-M39-GS) (gamma) vectors were obtained from GeneCopoeia.

Transfections were performed using Lipofectamine 2000 (Invitrogen, Thermo Fisher Scientific). For production of SARS-CoV-2 S-pseudotyped lentiviral (LV) particles carrying a firefly luciferase reporter gene, 293T cells were co-transfected with the Wuhan plasmid, the D614G plasmid, or plasmids encoding spike protein variants (alpha, beta, gamma, delta), the pCMVR 8.74 lentiviral packaging plasmid (a kind gift from R. Piva, University of Turin, Italy) and the pLenti CMV Puro LUC plasmid (Addgene plasmid #17477), a gift from Eric Campeau and Paul Kaufman.[35] At 48 h after transfection, supernatants containing the viral particles were collected, filtered through 0.45 μm membranes, and frozen at −80°C until use. Spike-pseudotyped LV titers were determined assessing the number of viral RNA genomes per milliliter using qRT-PCR. Briefly, viral RNAs extracted with TRIzol-LS Reagent (Invitrogen, Thermo Fisher Scientific) were digested with TURBO DNase (Invitrogen, Thermo Fisher Scientific) at 37°C for 15 min. Reverse transcription of viral RNA (5 μL) was performed using PrimeScript RT Reagent Kit (Takara). qRT-PCR analysis was carried out using a CFX-96 Touch Real-Time PCR Detection System (Bio-Rad) using the SensiFAST SYBR kit (Bioline) and primers specific for the luciferase-reporter gene (Luc F: 5′-CATTC CGGATACTGCGATTT-3′; Luc R: 5′-GGCGAAGAAGGAGAATA GGG-3′). To generate a standard curve, a 451 bp (positions 544–994) luciferase-RNA fragment was transcribed *in vitro* using MEGAshortscript T7 Transcription Kit (Invitrogen, Thermo Fisher Scientific). Pseudovirus particles were adjusted to the same titer (RNA copies per milliliter) in all neutralization experiments. For *in vivo* experiments, LV pseudotyped with the SARS-CoV-2 D614G-S variant was produced as described above, concentrated using PEG Virus Precipitation Kit (Abcam), resuspended in Abcam VR (virus re-suspension) solution, and then frozen at −80°C until use.

SARS-CoV-2 S-pseudovirus neutralization assay

Human Caco-2 hACE2 cells, stably expressing the hACE2 receptor, were grown at 37°C and 5% CO_2, in DMEM (Euroclone) supplemented with 10% FCS, 2 mM glutamine, and antibiotics. Generation of Caco-2 hACE2 cells has been described previously.[31] Caco-2 hACE2 cells were plated at a density of 3×10^4 cells/well in white, clear-bottom 96-well plates (Costar). After 24 h, 100 μL DMEM containing 5% FCS and 8 μg/mL polybrene were added to each well, and cells were incubated for 30 min. Serial (1:3) dilutions (range: from 1 μg/mL to 0.004 μg/mL final concentration) of scFvs were prepared in DMEM containing 5% FCS. Each dilution was tested in duplicate on each plate. Aliquots (60 μL) of the LV suspension were added to an equal amount of each antibody dilution (60 μL) and incubated for 1 h at 37°C. Pseudovirus:scFv mixtures (50 μL) were then added to Caco-2 hACE2 cells after medium removal. An additional 50 μL of DMEM containing 5% FCS was added to each well after 24 h. Luciferase activity (relative luciferase units [RLU]) was detected at 72 h post-infection by using Bright-Glo Luciferase Assay System Kit (Promega) in a Microplate Luminometer (Wallac-PerkinElmer).

Epitope mapping

Shotgun mutagenesis epitope mapping services were provided by Integral Molecular (Philadelphia, PA) as described by Davidson and Doranz (2014).[36] Briefly, a mutation library of the target protein was created using high-throughput, site-directed mutagenesis. Each residue was individually mutated to alanine, with alanine codons mutated to serine. The mutant library was arrayed in 384-well microplates and transiently transfected into HEK 293-T cells. Following transfection, cells were incubated with the indicated antibodies at concentrations pre-determined using an independent immunofluorescence titration curve on wild-type protein. Test antibodies were detected using an Alexa Fluor 488-conjugated secondary antibody, and mean cellular fluorescence was determined using Intellicyt iQue flow cytometry platform. Mutated residues were identified as being critical to the test antibody epitope if they did not support the reactivity of the test antibody but did support the reactivity of the reference MAb. This counterscreen strategy facilitates the exclusion of mutants that are locally misfolded or that have an expression defect.

Biochemical analyses

SDS-PAGE was performed using standard methods.[37] SEC-HPLC analyses were performed on an ALLIANCE HPLC system equipped with a 2998 Photodiode Array detector (Waters). Antibodies were loaded on a TSKgel G3000 SWXL 30 cm × 7.8 mm column (Tosoh Bioscience) at a concentration of 3 μg in 100 μL PBS and eluted with running buffer (50 mM phosphate buffer, 150 mM NaCl, pH 7.2), or running buffer/acetonitrile mixture (90:10 v/v), at a flow rate of 0.75 mL/min. Peaks were detected at 280 nm. For some analyses, antibodies were loaded on a BioSep 5 μM SEC-S2000 145 Å 300 × 7.8 mm column (PHENOMENEX) and eluted with running buffer or running buffer/acetonitrile mixture (90:10 v/v), at a flow rate of 1 mL/min. Detection was by 280 nM absorbance.

SEC-MS analysis was performed on an UHPLC Ultimate 3000SD (Thermo Fisher Scientific) coupled to a Q-Exactive Plus mass spectrometer (Thermo Fisher Scientific) operating in electrospray ionization in positive ion mode. The analysis was performed on a column Mab Pac SEC-1 (2.1 × 100 mm; Thermo Fisher Scientific), maintained at 25°C using 20 mM ammonium formate. The mass spectra were recorded from m/z 1500 to m/z 8000 in native conditions.

The primary amino acid sequences were confirmed by peptide mass fingerprint analysis. Samples were reduced, alkylated, and digested with trypsin. The resulting peptide mixtures were analyzed using RP-UHPLC-MS/MS. The samples were injected on a column Acquity UPLC Waters CSH C18 130Å (1 × 100 mm, 1.7 μm; Waters). The column oven was maintained at 55°C, and the analysis was carried using a gradient elution (phase A: 0.1% formic acid in water; phase B: 0.1% formic acid in acetonitrile). The flow rate was maintained at 0.1 mL/min. The mass spectra were acquired in "data-dependent scan" mode, able to acquire both the full mass spectra in high resolution and to isolate and fragment the ten ions with highest intensity present in the mass spectrum. The raw data obtained were analyzed using the Biopharma Finder 2.1 software (Thermo Fisher Scientific). The elaboration process consisted in the comparison between the peak list obtained "*in silico*" considering an expected amino acid sequence of a certain protein and fixed or variable modifications (carboamidomethylation, oxidation, etc.) and the experimental data.

Circular dichroism

CD experiments were performed on a Jasco J-815 spectropolarimeter equipped with a PTC-423S/15 Peltier temperature controller. Cells with 0.1 cm path length and scFv protein concentrations of 0.2–0.9 mg/mL were used to record CD spectra between 200 and 250 nm, with a 2 nm bandwidth and a scan rate of 5 or 20 nm/min. Spectra were recorded at 20°C and 90°C. Spectra were signal-averaged over five scans, baseline-corrected by subtracting a buffer spectrum, and smoothed using the means-movement function before conversion to molar ellipticity. Spectra were analyzed for secondary structure composition using the BeStSel method.[22]

In vivo models of infection with SARS-CoV-2 or SARS-CoV-2 S-pseudotyped virus

Animal studies were performed in accordance with the European Directive 2010/63/EU on the protection of animals used for scientific purposes, applied in Italy by the Legislative Decree 4 March 2014, n. 26. This study was included in a main research project approved by the Italian Department of Health. Female transgenic mice (K18-hACE2), aged 4–6 weeks, were infected via the intranasal route (10 μL/nostril) with an LV pseudotyped with the SARS-CoV-2 D614G-S variant expressing luciferase (Lenti-LUC-spike D614G), generated as described above. A luciferase-expressing lentivirus was used (10 μL/nostril) as a negative control. Two hours before and 4 h after infection, scFv76 (3.7 mg/mL in PBS) and scFv76-58 (2.6 mg/mL in PBS) antibodies were intranasally administered (10 μL/nostril and 14 μL/nostril, respectively) to mice (n = 12/group). An unrelated scFv (2.6 mg/mL in PBS) was also administered (14 μL/nostril) to additional mice (n = 12) in the same experimental conditions as above. At three different time points (48, 72, and 96 h post-infection) Lenti-LUC-spike D614G bioluminescence was quantitatively measured through the IVIS200 optical imaging system (PerkinElmer) for each mouse. Total body bioluminescence imaging was performed on mice before euthanasia, then explanted lungs and nasal turbinates were imaged. *In vivo* scFv testing against an authentic SARS-CoV-2 strain was performed by using a Golden Syrian hamster model at the François Hyafil Research Institute (Oncodesign, Villebon-sur-Yvette, France). Animal housing and experimental procedures were conducted according to the French and European Regulations and the National Research Council Guide for the Care and Use of Laboratory Animals. SARS-CoV-2 strain "Slovakia/SK-BMC5/2020," originally provided by the European Virus Archive global (EVAg) with D614G mutation, produced and tittered by Oncodesign on Vero E6/TMPRSS2 cells, was used for hamster infection. Female 7-week-old Golden Syrian hamsters, purchased from Janvier Labs, were anesthetized with isoflurane and inoculated intranasally with 70 μL (35 μL/nostril) containing a dose of 10^5 pfu SARS-CoV-2. ScFv76 (1 mg/mL in D-PBS) was administered by intranasal route to isoflurane-anesthetized animals (n = 5), under a volume of 70 μL (35 μL/nostril), 2 h before infection and then once daily for 2 consecutive days post-infection. Hamsters were monitored for appearance, behavior, and weight and ultimately were euthanized at day 4 post-infection by intraperitoneal injection of a cocktail of Zoletil (30 mg/kg) and xylazine (10 mg/kg) followed by gentle cervical dislocation. Thoracotomy was then performed before tissue collection and lung necropsy.

In vivo nebulization of 76clAbs

Animal studies were performed in accordance with the European Directive 2010/63/EU on the protection of animals used for scientific purposes, applied in Italy by the Legislative Decree 4 March 2014, n. 26. This study was included in a research project approved by Italian Department of Health.

Female BALB/c OlaHsd mice, purchased from Envigo, were nebulized with scFv antibodies at various concentrations (ranging from 1 to 5 mg/mL) in DPBS, and at different duration of nebulization exposure, by using homemade equipment, based on the Aerogen Pro (Aerogen) mesh nebulizer and a nose-only inhalation chamber, suitable for delivering the nebulized antibodies contemporarily up to 8 mice. At different time points post-nebulization mice were euthanized and lungs explanted and then fixed by 4% paraformaldehyde for immunohistochemical (IHC) analyses or snap-frozen (in liquid nitrogen) and stored at −80°C until further analysis.

To assess the recovery of functional scFv antibody, the snap-frozen lungs were weighed, transferred to different tubes on ice in the presence of 1× Lysis buffer (Cell Signaling Technology), already containing different protease inhibitors and supplemented with 1 mM PMSF. The lung tissues were homogenized at 4°C for 20 s through a rotor-stator homogenizer, then incubated on ice for 15 min and sonicated for 30 s by a suitable ultrasonic bath. Lung homogenates were centrifuged at 14,000 × *g* for 10 min at 4°C, and then supernatants were transferred to clean microcentrifuge tubes and frozen on dry ice and stored at −80°C. Total protein concentrations in the lung tissue homogenates were determined using a classical Bradford assay. To test whether the nebulized antibodies conserved their functional properties, aliquots of lung tissue homogenates were diluted in PBS buffer containing Tween and BSA and then assessed by ELISA for the binding to SARS-CoV-2 RBD as previously described.

Immunohistochemistry

Immunohistochemistry staining to detect the scFv antibodies in mice lungs after nebulization was performed by using the anti-His tag antibody rabbit monoclonal antibody, clone RM146 (catalog no. SAB5600227; Sigma-Aldrich). Briefly, slides were deparaffinized and treated with 3% H_2O_2 in H_2O to quench endogenous peroxidase activity. Staining of scFv antibodies with the primary anti-His tag antibody was performed at 4°C ON, followed by exposure to biotinylated-anti-rabbit secondary antibody for 60 min at room temperature. Diaminobenzidine (DAB) was used as the chromogen. Microscopic observation was performed using a Nikon Eclipse 80i microscope equipped with a DXM1200F Microscope Camera. Cross-reactivity of scFv76 with human normal tissues was assessed by using tissue microarrays (TMAs), obtained from US Biomax (catalog no. MN0341). To this end, slides were treated as described above and then incubated with scFv (10 μg/mL) overnight at 4°C, followed by the same procedures described before. An anti-hPDL1 scFv was used as positive control.

Statistical analysis

Statistical analyses were performed using GraphPad Prism software (version 6.0 or 8.0). Data are presented as average ± SE or average ± SD. Statistical analyses were carried out using unpaired two-tailed Student's t tests or one-way ANOVA. p values less than 0.05 were considered to indicate statistical significance.

SUPPLEMENTAL INFORMATION

Supplemental information can be found online at https://doi.org/10.1016/j.ymthe.2022.02.013.

ACKNOWLEDGMENTS

We are grateful to COVID-19 convalescent subjects for providing blood samples. We thank Integral Molecular (Philadelphia) for expedite identification of the antibody epitope; Dr. Silvia Santopolo for help with pseudovirus RNA titration; Dr. Nestor Santiago Gonzalvo (Cytiva) for excellent technical assistance on Biacore analyses; Claudio Albertoni and Evelyn Vaccaro for expert technical assistance in animal models; and Prof. Luigi Giusto Spagnoli for expert opinion on immunohistochemistry. Data and materials availability: antibodies described in the paper can be provided upon material transfer agreement (MTA) subscription.

AUTHOR CONTRIBUTIONS

Conceptualization, G.G., G. Borleri, A. Rambaldi, M.G.S., E.M.P., O.M., and R.D.S.; Investigation, D.S., A.M.A., F.M., B.P., G. Battistuzzi, L.S., C.C., A. Rosi, C.D., C.V., A. Rossi, L.L., and A. Riccio; Supervision and Manuscript Writing, M.G.S., E.M.P., and R.D.S.

DECLARATION OF INTERESTS

O.M., E.M.P., and R.D.S. are employees of Alfasigma SpA and are named as inventors on a patent application in the name of the same company.

REFERENCES

1. Krause, P.R., Fleming, T.R., Longini, I.M., Peto, R., Briand, S., Heymann, D.L., Beral, V., Snape, M.D., Rees, H., Ropero, A.M., et al. (2021). SARS-CoV-2 variants and vaccines. N. Engl. J. Med. *385*, 179–186.
2. Bernal, J.L., Andrews, N., Gower, C., Gallagher, E., Simmons, R., Thelwall, S., Stowe, J., Tessier, E., Groves, N., Dabrera, G., et al. (2021). Effectiveness of covid-19 vaccines against the B.1.617.2 (delta) variant. N. Engl. J. Med. *385*, 585–594.
3. Wise, J. (2021). Covid-19: delta variant doubles risk of hospital admission compared with alpha variant, study shows. Br. Med. J. *374*, n2152.
4. Papageorgiou, A.C., and Mohsin, I. (2020). The SARS-CoV-2 spike glycoprotein as a drug and vaccine target: structural insights into its complexes with ACE2 and antibodies. Cells *9*, 2343.
5. Santopolo, S., Riccio, A., and Santoro, M.G. (2021). The biogenesis of SARS-CoV-2 spike glycoprotein: multiple targets for host-directed antiviral therapy. Biochem. Biophys. Res. Commun. *538*, 80–87.
6. Taylor, P.C., Adams, A.C., Hufford, M.M., de la Torre, I., Winthrop, K., and Gottlieb, R.L. (2021). Neutralizing monoclonal antibodies for treatment of COVID-19. Nat. Rev. Immunol. *21*, 382–393.
7. Kreuzberger, N., Hirsch, C., Chai, K.L., Tomlinson, E., Khosravi, Z., Popp, M., Neidhardt, M., Piechotta, V., Salomon, S., Valk, S.J., et al. (2021). SARS-CoV-2-neutralising monoclonal antibodies for treatment of COVID-19. Cochrane Database Syst. Rev. *9*, cd013825.
8. Planas, D., Veyer, D., Baidaliuk, A., Staropoli, I., Guivel-Benhassine, F., Rajah, M.M., Planchais, C., Porrot, F., Robillard, N., Puech, J., et al. (2021). Reduced sensitivity of SARS-CoV-2 variant Delta to antibody neutralization. Nature *596*, 276–280.
9. Liu, Y., Soh, W.T., Kishikawa, J.I., Hirose, M., Nakayama, E.E., Li, S., Sasai, M., Suzuki, T., Tada, A., Arakawa, A., et al. (2021). An infectivity-enhancing site on the SARS-CoV-2 spike protein targeted by antibodies. Cell *184*, 3452–3466.e18.
10. Zhou, D., Chan, J.F.W., Zhou, B., Zhou, R., Li, S., Shan, S., Liu, L., Zhang, A.J., Chen, S.J., Chan, C.C.S., et al. (2021). Robust SARS-CoV-2 infection in nasal turbinates after treatment with systemic neutralizing antibodies. Cell Host Microbe *4*, 551–563.e5.
11. Cruz-Terana, C., Tiruthani, K., McSweeney, M., Ma, A., Pickles, R., and Lai, S.K. (2021). Challenges and opportunities for antiviral monoclonal antibodies as COVID-19 therapy. Adv. Drug Deliv. Rev. *169*, 100–117.
12. Xu, J., Xu, K., Jung, S., Conte, A., Lieberman, J., Muecksch, F., Cetrulo Lorenzi, J.C., Park, S., Schmidt, F., Wang, Z., et al. (2021). Nanobodies from camelid mice and llamas neutralize SARS-CoV-2 variants. Nature *595*, 278–282.
13. Nambulli, S., Xiang, Y., Tilston-Lunel, N.L., Rennick, L.J., Sang, Z., Klimstra, W.B., Reed, D.S., Crossland, N.A., Shi, Y., and Duprex, W.P. (2021). Inhalable Nanobody (PiN-21) prevents and treats SARS-CoV-2 infections in Syrian hamsters at ultra-low doses. Sci. Adv. *7*, eabh0319.
14. Wiswell, D., Neupane, D., Chen, M., Bowman, E.P., Linn, D., Sawant, A., Chackerian, A., Zhang, S., and Escandón, E. (2020). A capillary electrophoresis-based approach for the identification of anti-drug antibodies against camelid VHH biologics (Nanobodies®). J. Pharmacol. Toxicol. Methods *103*, 106872–106880.
15. Huston, J.S., Levinson, D., Mudgett-Hunter, M., Tai, M.S., Novotny, J., Margolies, M.N., Ridge, R.J., Bruccoleri, R.E., Haber, E., and Crea, R. (1988). Protein engineering of antibody binding sites: recovery of specific activity in an anti-digoxin single-chain Fv analogue produced in Escherichia coli. Proc. Natl. Acad. Sci. U S A *85*, 5879–5883.
16. Markham, A. (2019). Brolucizumab: first approval. Drugs *79*, 1997–2000.
17. Bussani, R., Schneider, E., Zentilin, L., Collesi, C., Ali, H., Braga, L., Volpe, M.C., Colliva, A., Zanconati, F., Berlot, G., et al. (2020). Persistence of viral RNA, pneumocyte syncytia and thrombosis are hallmarks of advanced COVID-19 pathology. EBioMedicine *61*, 103104.
18. Cameroni, E., Bowen, J.E., Rosen, L.E., Saliba, C., Zepeda, S.K., Culap, K., Pinto, D., VanBlargan, L.A., De Marco, A., di Iulio, J., et al. (2021). Broadly neutralizing antibodies overcome SARS-CoV-2 Omicron antigenic shift. Nature. https://doi.org/10.1038/s41586-021-04386-2.
19. Planas, D., Saunders, N., Maes, P., Guivel-Benhassine, F., Planchais, C., Buchrieser, J., Bolland, W.H., Porrot, F., Staropoli, I., Lemoine, F., et al. (2021). Considerable escape of SARS-CoV-2 Omicron to antibody neutralization. Nature. https://doi.org/10.1038/s41586-021-04389-z.

20. Wang, P., Nair, M.S., Liu, L., Iketani, S., Luo, Y., Guo, Y., Wang, M., Yu, J., Zhang, B., Kwong, P.D., et al. (2021). Antibody resistance of SARS-CoV-2 variants B.1.351 and B.1.1.7. Nature *593*, 130–135.

21. Chen, R.E., Winkler, E.S., Case, J.B., Aziati, I.D., Bricker, T.L., Joshi, A., Darling, T.L., Ying, B., Errico, J.M., Shrihari, S., et al. (2021). In vivo monoclonal antibody efficacy against SARS-CoV-2 variant strains. Nature *596*, 103–108.

22. Micsonai, A., Wien, F., Kernya, L., Lee, Y.H., Goto, Y., Réfrégiers, M., and Kardos, J. (2015). Accurate secondary structure prediction and fold recognition for circular dichroism spectroscopy. Proc. Natl. Acad. Sci. U S A *112*, E3095–E3103.

23. Vojdani, A., Vojdani, E., and Kharrazian, D. (2021). Reaction of human monoclonal antibodies to SARS-CoV-2 proteins with tissue antigens: implications for autoimmune diseases. Front. Immunol. *11*, 617089.

24. Hastie, K.M., Li, H., Bedinger, D., Schendel, S.L., Dennison, S.M., Li, K., Rayaprolu, V., Yu, X., Mann, C., Zandonatti, M., et al. (2021). Defining variant-resistant epitopes targeted by SARS-CoV-2 antibodies: a global consortium study. Science *374*, 472–478.

25. Lai, S.K., McSweeney, M.D., and Pickles, R.J. (2021). Learning from past failures: challenges with monoclonal antibody therapies for COVID-19. J. Control. Release *329*, 87–95.

26. Piano Mortari, E., Russo, C., Vinci, M.R., Terreri, S., Salinas, A.F., Piccioni, L., Alteri, C., Colagrossi, L., Coltella, L., Ranno, S., et al. (2021). Highly-specific memory B cells generation after the 2nd dose of BNT162b2 vaccine compensate for the decline of serum antibodies and absence of mucosal IgA. Cells *10*, 2541.

27. Pavoni, E., Monteriù, G., Santapaola, D., Petronzelli, F., Anastasi, A.M., Pelliccia, A., D'Alessio, V., De Santis, R., and Minenkova, O. (2007). Tumor-infiltrating B lymphocytes as an efficient source of highly specific immunoglobulins recognizing tumor cells. BMC Biotechnol. *7*, 70–86.

28. Pavoni, E., and Minenkova, O. (2007). Vector for efficient selection and/or maturation of an antibody and uses thereof (European Patent Office). WO2007/074496.

29. Pavoni, E., Monteriù, G., Cianfriglia, M., and Minenkova, O. (2007). New display vector reduces biological bias for expression of antibodies in E. coli. Gene *391*, 120–129.

30. Ramakrishnan, M.A. (2016). Determination of 50% endpoint titer using a simple formula. World J. Virol. *5*, 85–86.

31. Riccio, A., Santopolo, S., Rossi, A., Piacentini, S., Rossignol, J.F., and Santoro, M.G. (2021). Impairment of SARS-CoV-2 spike-glycoprotein maturation and fusion-activity by nitazoxanide: an effect independent of spike variants emergence. Preprint at bioRxiv. https://doi.org/10.1101/2021.04.12.439201.

32. Zhang, L., Jackson, C.B., Mou, H., Ojha, A., Peng, H., Quinlan, B.D., Rangarajan, E.S., Pan, A., Vanderheiden, A., Suthar, M.S., et al. (2020). SARS-CoV-2 spike-protein D614G mutation increases virion spike density and infectivity. Nat. Commun. *11*, 6013–6021.

33. Ou, X., Liu, Y., Lei, X., Li, P., Mi, D., Ren, L., Guo, L., Guo, R., Chen, T., Hu, J., et al. (2020). Characterization of spike glycoprotein of SARS-CoV-2 on virus entry and its immune cross-reactivity with SARS-CoV. Nat. Commun. *11*, 1620–1631.

34. Buchrieser, J., Dufloo, J., Hubert, M., Monel, B., Planas, D., Rajah, M.M., Planchais, C., Porrot, F., Benhassine, F.G., Van der Werf, S., et al. (2020). Syncytia formation by SARS-CoV-2-infected cells. EMBO J. *39*, e106267.

35. Campeau, E., Ruhl, V.E., Rodier, F., Smith, C.L., Rahmberg, B.L., Fuss, J.O., Campisi, J., Yaswen, P., Cooper, P.K., and Kaufman, P.D. (2009). A versatile viral system for expression and depletion of proteins in mammalian cells. PLoS One *4*, e6529.

36. Davidson, E., and Doranz, B.J. (2014). A high-throughput shotgun mutagenesis approach to mapping B-cell antibody epitope. Immunology *143*, 13–20.

37. Maniatis, T., Fritsch, E.F., and Sambrook, J. (1982). Molecular Cloning: A Laboratory Manual (Cold Spring Harbor).